Deep-Sea Research II 56 (2009) 964–976

Contents lists available at ScienceDirect

Deep-Sea Research II

journal homepage: www.elsevier.com/locate/dsr2

Nitrous oxide and methane in the Atlantic Ocean between 50°N and 52°S: Latitudinal distribution and sea-to-air flux

Grant Forster [a,*], Rob C. Upstill-Goddard [a], Niki Gist [b], Carol Robinson [b,1], Gunther Uher [a], E. Malcolm S. Woodward [b]

[a] Ocean Research Group, School of Marine Science and Technology, University of Newcastle upon Tyne, Newcastle upon Tyne NE1 7RU, UK
[b] Plymouth Marine Laboratory, Prospect Place, Plymouth PL1 3DH, UK

ARTICLE INFO

Available online 9 December 2008

Keywords:
Nitrous oxide
Methane
Atlantic Ocean
Depth Profile
Gas Exchange
Ocean atmosphere interaction

ABSTRACT

We discuss nitrous oxide (N_2O) and methane (CH_4) distributions in 49 vertical profiles covering the upper ~300 m of the water column along two ~13,500 km transects between ~50°N and ~52°S during the Atlantic Meridional Transect (AMT) programme (AMT cruises 12 and 13). Vertical N_2O profiles were amenable to analysis on the basis of common features coincident with Longhurst provinces. In contrast, CH_4 showed no such pattern. The most striking feature of the latitudinal depth distributions was a well-defined "plume" of exceptionally high N_2O concentrations coincident with very low levels of CH_4, located between ~23.5°N and ~23.5°S; this feature reflects the upwelling of deep waters containing N_2O derived from nitrification, as identified by an analysis of N_2O, apparent oxygen utilization (AOU) and NO_3^-, and presumably depleted in CH_4 by bacterial oxidation. Sea-to-air emissions fluxes for a region equivalent to ~42% of the Atlantic Ocean surface area were in the range 0.40–0.68 Tg N_2O yr^{-1} and 0.81–1.43 Tg CH_4 yr^{-1}. Based on contemporary estimates of the global ocean source strengths of atmospheric N_2O and CH_4, the Atlantic Ocean could account for ~6–15% and 4–13%, respectively, of these source totals. Given that the Atlantic Ocean accounts for around 20% of the global ocean surface, on unit area basis it appears that the Atlantic may be a slightly weaker source of atmospheric N_2O than other ocean regions but it could make a somewhat larger contribution to marine-derived atmospheric CH_4 than previously thought.

1. Introduction

Nitrous oxide (N_2O) and methane (CH_4) both strongly influence Earth's climate and atmospheric chemistry. They have relatively long atmospheric lifetimes and are infrared-active; together they account for ~20% of enhanced greenhouse forcing (IPCC, 2001). N_2O participates in stratospheric O_3 regulation via NO_x generation (Nevison and Holland, 1997) and CH_4 is involved in the formation of stratospheric water and in photochemical reactions that regulate tropospheric OH and O_3 (Crutzen, 1991). The atmospheric inventories of N_2O and CH_4 are currently increasing, but at variable rates that are not well understood (Dlugokencky et al., 1998, 2001; Khalil and Rasmussen, 1992; Prinn et al., 1990) hence their global source–sink functions are the subject of intense scrutiny (IPCC, 2001).

The marine sources of N_2O and CH_4 are not well constrained. For CH_4 one estimate sets this at 0.4 Tg CH_4 yr^{-1} (Bates et al., 1996) although most recent syntheses converge at around 11–18 Tg CH_4 yr^{-1}, about 2–3% of the global total (e.g. Bange et al., 1994; Lelieveld et al., 1998). Importantly, Bange et al. (1994) attribute ~75% of the latter estimate to estuarine and shelf sea sources. For N_2O the uncertainty is no better; recent estimates suggest 6.28 Tg N_2O yr^{-1} (range 1.99–10.68 Tg N_2O yr^{-1}) (Nevison et al., 1995) and 4.71 Tg N_2O yr^{-1} (range 1.57–7.85 Tg N_2O yr^{-1}) (Mosier et al., 1998; Kroeze et al., 1999) against a global source total ~25.8 Tg N_2O yr^{-1} (IPCC, 2001). However, Bange (2006) suggests that these estimates of the oceanic N_2O source strength are too low and that ~11 ±6.28 Tg N_2O yr^{-1} is more realistic. As for CH_4, this higher estimate is believed to be dominated by coastal N_2O sources (Bange et al., 1996; Bange, 2006). The uncertainty surrounding the marine sources of N_2O and CH_4 reflects a paucity of targeted sampling in key marine provinces. Perhaps somewhat surprisingly, much of the South Atlantic Ocean remains poorly sampled with respect to subsurface N_2O and CH_4. Weiss et al. (1992) measured N_2O in 6 N. Atlantic, 4 Tropical Atlantic, and 9 S. Atlantic surface transects between 1978 and 1990. N_2O was highest in the tropical and Benguela upwellings (~120–130% saturation), whereas the N and S Atlantic ranged from mildly undersaturated to moderately supersaturated in N_2O (Weiss et al., 1992). Butler et al. (1995) collected 40 Atlantic N_2O depth profiles,

* Corresponding author.
E-mail address: G.forster@uea.ac.uk (G. Forster).
[1] Current address: School of Environmental Sciences, University of East Anglia, Norwich NR4 7TJ, UK.

0967-0645/$ - see front matter Crown Copyright © 2008 Published by Elsevier Ltd. All rights reserved.
doi:10.1016/j.dsr2.2008.12.002

35 of which were in the South Atlantic between the equator and ~50°S, along a south-westerly transect between ~25 and ~30°W. Concentrations throughout the top 100 m were in the range ~5–10 nmol N_2O L^{-1} (Butler et al., 1995; Nevison et al., 2003). For CH_4 Conrad and Seiler (1988) profiled from 35°S to 50°N; CH_4 saturations were in the range 101–158%. Rhee (2000) measured surface underway N_2O and CH_4 between the UK and Uruguay; both were mildly supersaturated with the exception of higher N_2O and CH_4 in the W. African Upwelling between the equator and 20°N. To our knowledge Rhee (2000) is the only study to date to include CH_4 measurements in the South Atlantic Gyre (SAG); however, these data are restricted to the upper 10 m (Rhee, 2000). Most other recent work has tended to focus on the tropical and sub-tropical North Atlantic (e.g. Oudot et al., 1990, 2002; Seifert et al., 1999; Morell et al., 2001; Walter et al., 2004, 2006). With the exception of surface data (e.g. Weiss et al., 1992; Rhee, 2000) N_2O and CH_4 distributions in the Atlantic Ocean remain incompletely described. This is important given that the Atlantic incorporates a range of oceanographic regimes, including both coastal and equatorial upwelling, oligotrophic gyres, high-nutrient low-chlorophyll (HNLC) waters, and high productivity waters with strong seasonal effects such as in the North Atlantic Spring bloom.

The Atlantic Meridional Transect Programme (AMT), which exploits the annual transit of RRS *James Clark Ross* between the UK and Antarctica in September–October and the return leg (Antarctica–UK) in April–May, offered a unique opportunity to investigate the distributions of N_2O and CH_4 in a range of Atlantic waters down to ~300 m, including temperate shelf seas, upwelling regions, and oligotrophic mid-ocean gyres (Hooker et al., 2000). The rationale and methodology of the AMT programme (2002–2006) and an overview of hydrographic conditions along the cruise tracks are presented elsewhere (Robinson et al., 2006). Here we report the distributions of N_2O and CH_4 in 49 vertical profiles covering the upper ~300 m of the water column along two ~13,500 km transects between ~50°N and ~52°S (AMT cruises 12 and 13). Importantly our measurements include novel data from the SAG. Our complete data set provides a basis for deriving gyre scale sea-to-air-fluxes of N_2O and CH_4 and hence for re-evaluating the contribution from the Atlantic Ocean to the atmospheric budgets of these climatically important gases.

2. Methods

2.1. Cruise tracks

The AMT12 (12 April–17 May 2003) and AMT13 (10 September–14 October 2003) cruise tracks (Fig. 1) were designed to meet the overarching AMT objectives of evaluating intra- and inter-annual variability in biogeochemical processes in the mid-North and South Atlantic Gyres, to compare ecosystem functioning between the gyres, and to sample climatically active trace gases (Robinson et al., 2006). The two cruises together crossed a total of 7 biogeographical provinces defined by Longhurst (1998) on the basis of satellite (CZCS) imagery supported by near-surface hydrography, light and nutrient distributions, plankton ecology, and other measurements (Fig. 1, Table 1): South Subtropical Convergence (SSTC, 45–42°S); South Atlantic Gyral (SATL, 42–6°S); Western Tropical Atlantic (WTRA, 6°S–11°N); North Atlantic Tropical Gyral (NATR, 11–26°N); North Atlantic Subtropical Gyral—East (NAST(E), 26–44°N); North Atlantic Drift (NADR, 44–58°N); Eastern (Canary) Coastal (CNRY, 13–26°S). Common to both cruises was sampling between the equator and 30°S primarily along 25°W in the SAG, which affords some degree of seasonal data comparison for this region. In contrast, the northern hemisphere cruise tracks were very different. While AMT12 sampled along a SW–SE zigzag into the North Atlantic Gyre (NAG) with the most westerly station at 35.83°W, AMT13 targeted coastal upwelling off the Moroccan and Mauritanian shelf (Fig. 1). General hydrographic aspects and some relevant biogeochemical features along the cruise tracks have already been reported (Robinson et al., 2006).

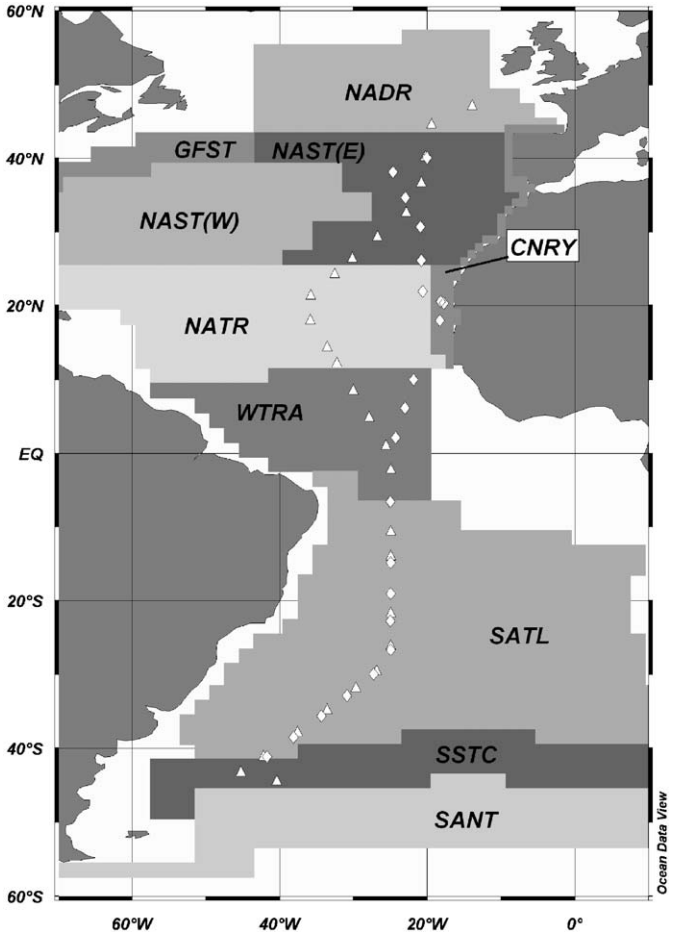

Fig. 1. AMT12 (white triangles) and AMT13 (white diamonds) cruise tracks shown in relation to Longhurst (1998) province. North Atlantic Drift Province (NADR), North Atlantic Subtropical Gyral Province (NAST), Gulf Stream Province (GFST), North Atlantic Tropical Gyral Province (NATR), Western Tropical Atlantic Province (WTRA), South Atlantic Gyral province (SATL), South Subtropical Convergence Zone (SSTC), Subantarctic Water Ring Province (SANT), Eastern (Canary) Coastal Province (CNRY).

2.2. Sampling

Water samples for dissolved N_2O, CH_4, O_2, and NO_3^- were collected predawn (0200–0400 h, local time) with a standard CTD (Sea-Bird 911 *plus*) rosette (Ocean Test Equipment: 24 × 20 L Niskins). Sampling dates, locations and depths are summarized in Table 1; sampling always routinely included the chlorophyll maximum and the following percentage irradiances: 97, 55, 33, 14, 1.0 and 0.1 (Robinson et al., 2006).

Sub-samples for dissolved gas analyses were always the first to be drawn from the CTD (typically 9–10 per cast); collection was via silicon tubing. In each case care was taken to avoid air entrainment and the sample was allowed to overflow by three volumes. Single samples for N_2O and CH_4 analyses were collected in 1 L volumetric flasks and immediately poisoned with 200 μL of 0.25 M aqueous $HgCl_2$. Selected dissolved O_2 samples were

Table 1
Stations sampled during AMT12 and AMT13.

Station	Date/time (GMT)	Latitude	Longitude	Depth (m)	MLD (m)
AMT12 5	16/05/2003 07:52	44.4193°S	40.3679°W	304	76
AMT12 7	17/05/2003 07:38	43.1983°S	45.3017°W	307	75
AMT12 10	18/05/2003 07:44	41.0481°S	42.1586°W	305	77
AMT12 12	19/05/2003 07:01	37.7904°S	37.6164°W	303	91
AMT12 14	20/05/2003 07.16	34.7802°S	33.5790°W	302	80
AMT12 16	21/05/2003 06:58	31.7853°S	29.7094°W	302	81
AMT12 19	22/05/2003 06:36	29.5249°S	26.8882°W	302	66
AMT12 21	23/05/2003 06:40	26.0542°S	25.0066°W	301	77
AMT12 23	24/05/2003 06:37	21.6291°S	25.0010°W	301	74
AMT12 26	26/05/2003 06:39	13.9263°S	24.9975°W	303	75
AMT12 29	27/05/2003 06:37	10.5969°S	24.9972°W	303	76
AMT12 33	29/05/2003 06:05	02.2361°S	24.9991°W	302	22
AMT12 36	30/05/2003 06:14	01.0867°N	25.6463°W	303	33
AMT12 38	31/05/2003 06:08	04.8951°N	27.8908°W	302	8
AMT12 40	01/06/2003 06:07	08.5325°N	30.0579°W	302	45
AMT12 42	02/06/2003 06:06	12.2343°N	32.2863°W	302	58
AMT12 45	03/06/2003 06:06	14.4251°N	33.6071°W	303	46
AMT12 47	04/06/2003 06:04	18.0365°N	35.8293°W	303	38
AMT12 49	05/06/2003 06:07	21.4140°N	35.8022°W	304	45
AMT12 51	06/06/2003 06:06	24.3287°N	32.5738°W	303	60
AMT12 54	07/06/2003 05:34	26.4607°N	30.1621°W	304	28
AMT12 56	08/06/2003 05:05	29.3887°N	26.7853°W	303	18
AMT12 58	09/06/2003 05:04	32.6815°N	22.8661°W	304	12
AMT12 60	10/06/2003 05:06	36.7358°N	20.8141°W	303	18
AMT12 63	11/06/2003 05:04	40.2229°N	20.2379°W	303	28
AMT12 65	12/06/2003 04:03	44.6311°N	19.4542°W	303	35
AMT12 67	13/06/2003 04:06	47.1416°N	13.9385°W	305	33
AMT13 10	17/09/2003 03:57	40.0619°N	20.0146°W	303	39
AMT13 13	18/09/2003 00:54	38.1667°N	24.7006°W	303	17
AMT13 15	19/09/2003 03:24	34.6825°N	22.9930°W	305	32
AMT13 18	20/09/2003 03:36	30.7499°N	20.9413°W	304	40
AMT13 21	21/09/2003 05:01	26.1714°N	20.7985°W	305	43
AMT13 24	22/09/2003 04:32	21.9618°N	20.6302°W	305	28
AMT13 27	23/09/2003 04:48	20.5974°N	18.1603°W	304	15
AMT13 28	23/09/2003 12:15	20.3269°N	17.7707°W	303	14
AMT13 30	24/09/2003 04:33	18.0049°N	18.2847°W	303	14
AMT13 34	26/09/2003 04:43	09.9567°N	21.8573°W	300	30
AMT13 37	27/09/2003 04:38	06.1359°N	23.0641°W	303	43
AMT13 40	28/09/2003 04:45	02.1565°N	24.3170°W	305	73
AMT13 44	30/09/2003 04:49	06.5634°S	25.0127°W	303	82
AMT13 50	02/10/2003 04:50	14.8232°S	25.0029°W	305	28
AMT13 53	03/10/2003 04:30	19.0339°S	25.0000°W	304	20
AMT13 56	04/10/2003 04:39	22.6946°S	25.0159°W	305	78
AMT13 59	05/10/2003 04:35	26.6455°S	25.0079°W	304	111
AMT13 62	06/10/2003 04:48	29.9501°S	27.3198°W	305	140
AMT13 65	07/10/2003 04:41	32.8845°S	30.9262°W	304	110
AMT13 68	08/10/2003 04:42	35.6198°S	34.3548°W	305	260
AMT13 71	09/10/2003 05:45	38.4817°S	38.1196°W	305	227
AMT13 74	10/10/2003 05:27	41.1514°S	41.7088°W	306	170

collected in gravimetrically calibrated 120 mL borosilicate glass bottles and immediately fixed with $MnSO_4$ and NaOH+NaI; these samples were used to calibrate an O_2 sensor (Sea-Bird Electronics, SBE 43) mounted on the CTD frame and used for routine dissolved O_2 measurements. Sub-samples for NO_3^- analysis were collected in acid-cleaned high-density polyethylene screw cap bottles following flushing with sample. Sample storage for N_2O and CH_4, and NO_3^- was in the dark in a 5 °C cold room. Pre-analysis storage never exceeded 8 h for N_2O and CH_4, and 4 h for NO_3^-. Samples for O_2 analysis were stored under water and analysed within 4-8 h of collection.

2.3. Analysis

Dissolved N_2O and CH_4 were analysed by single-phase equilibration gas chromatography, with electron capture detection (ECD) for N_2O and flame ionization detection (FID) for CH_4. Routine calibration was with a mixed secondary standard (361 ppbv N_2O, 2000 ppbv CH_4) prepared by pressure dilution (Upstill-Goddard et al., 1990, 1996) and independently calibrated against two mixed primary standards with certified accuracies of ±1% (10 ppmv N_2O, 5 ppmv CH_4 and 20 ppmv N_2O, 8 ppmv CH_4; BOC Special Gases, UK). Due to difficulties in obtaining mixed primary standards with suitably low N_2O mixing ratios we also used a 1.05 ppmv primary N_2O standard (certified accuracy ±2%) obtained from the National Physical Laboratory, New Delhi, India (http://www.nplindia.org/). Method analytical precision (1σ), determined from repeat analyses ($n = 10$) of the mixed secondary standard, was ±5%.

Equilibrated mixing ratios corrected for phase partitioning during analysis (Upstill-Goddard et al., 1996) were converted to percent saturations using atmospheric N_2O and CH_4 mixing ratios obtained from the Global Monitoring Division (GMD; http://www.esrl.noaa.gov/gmd/) of the National Oceanic and Atmospheric Administration/Earth System Research Laboratory

Table 2
Mixing ratios of N_2O and CH_4 at atmospheric monitoring stations during AMT12 and AMT13.

Station	Latitude	Longitude	Parameter	Atmospheric mixing ratio (ppbv)			
				CH_4 (June)	CH_4 (September)	N_2O (June)	N_2O (September)
Northern stations							
Alert	82.27	−62.31	CH_4, N_2O	1821	1833	318	317
Summit	72.35	−38.29	CH_4	1815	1832	–	–
Heimaey	63.20	−20.70	CH_4	1826	1831	–	–
Mace Head	53.20	−09.54	CH_4, N_2O	1820	1828	319	318
Harvard Forest	42.54	−72.18	N_2O	–	–	318	318
Tercia Island	38.46	−27.23	CH_4	1800	1820	–	–
Tudor Hill	32.16	−64.53	CH_4	1770	1823	–	–
Tenerife	28.18	−16.29	CH_4	1777	1780	–	–
Ragged Point	13.10	−59.26	CH_4, N_2O	1792	1801	318	318
Average				1803±21	1819±19	318±1	318±1
Southern stations							
Ascension Island	−07.55	−14.25	CH_4	1723	1726	–	–
Gobabeb	−23.35	15.02	CH_4	1679	1679	–	–
Cape Point	−34.21	18.29	CH_4, N_2O	1708	1720	317	317
Tierra Del Fuego	−54.52	−68.29	CH_4	1708	1707	–	–
Palmer Station	−64.55	−64.00	CH_4	1703	1722	–	–
Halley Bay	−75.35	−26.30	CH_4	1700	1722	–	–
South Pole	−89.59	−24.48	CH_4, N_2O	1702	1722	317	317
Average				1703±13	1714±17	317	317

All data are from the NOAA/ESRL with the exception of Cape Point where mixing ratios were obtained from SAWS.

Table 3
Mean mixed layer concentration of N_2O and CH_4 by Longhurst province for AMT12 and AMT13.

Province	AMT12				AMT13			
	Mean N_2O		Mean CH_4		Mean N_2O		Mean CH_4	
	% Saturation	nmol L^{-1}	% Saturation	nmol L^{-1}	% Saturation	nmol L^{-1}	% Saturation	nmol L^{-1}
SSTC	107±6	9.7±0.5	157±40	3.6±0.9	n.s.	n.s.	n.s.	n.s.
SATL	104±11	6.8±1	162±31	3±0.5	101±4	7.4±1	141±19	3.3±1.7
WTRA	109±21	5.9±1.3	176±43	3.5±0.8	106±7	5.7±0.4	133±33	2.9± 0.3
NATR	104±3	6.1±0.5	198±43	3.7±1	97±4	5.7±0.3	116±3	2.1±0.1
NAST (E)	105±8	7.1±0.7	185±50	3.7±0.9	102±4	6±0.5	120±11	2.2±0.2
NADR	98±10	7.6±0.9	147±17	3.3±0.4	n.s.	n.s.	n.s.	n.s.
CNRY	n.s.	n.s.	n.s.	n.s.	140±10	8.5±1.1	156±29	3±0.7

n.s. refers to not sampled.

(NOAA/ESRL), formerly the Climate Monitoring and Diagnostic Laboratory (CMDL) and from the Climate Division of the South African Weather Service (SAWS; http://www.weathersa.co.za) (Table 2). Dissolved concentrations were determined from corresponding partial pressures using solubility data from Weisenburg and Guinasso (1979) for CH_4 and Weiss and Price (1980) for N_2O.

Dissolved NO_3^- analysis was by one of two segmented flow colorimetric methods depending upon the anticipated concentration ranges. For samples $>1\,\mu mol\,L^{-1}$ NO_3^- analysis was on a Technicon AAII autoanalyser following the method of Brewer and Riley (1965) whereas samples $<1\,\mu mol\,L^{-1}$ NO_3^- were analysed in a long path-length (2 m) liquid waveguide capillary cell (Woodward, 2002). For both methods detection limits were $1.00\pm0.06\,nmol\,L^{-1}$ and overall precisions (1σ) were ±2%. Dissolved O_2 analysis was by automated Winkler titration; analytical precision (1σ) was better than ±1% (Williams and Jenkinson, 1982). Data were converted to percent O_2 saturations according to Benson and Krause (1984). Apparent oxygen utilization (AOU) was calculated as the difference between the *in situ* O_2 concentration and its theoretical O_2 concentration equivalent to 100% O_2 saturation (Weiss, 1970).

2.4. Mixed layer depths

Mixed layer depths required for estimating sea-to-air fluxes of N_2O and CH_4 were estimated from profiles of σ_θ and temperature (Hooker et al., 2000). We thus defined the base of the mixed layer as coinciding with the start of the thermocline as indicated by three out of four successive gradients in σ_θ and/or temperature exceeding $0.035\,m^{-1}$ and/or $0.1\,^\circ C\,m^{-1}$, respectively. For situations where the thermocline was too weak to be identified with this approach we assumed its top to be represented by a change of 0.1 in σ_θ or 0.5 °C in temperature relative to the corresponding surface value (after Hooker et al., 2000) (Table 1).

3. Results and discussion

3.1. N_2O and CH_4 in the upper 300 m

Table 3 lists mean mixed layer concentrations and percent saturations of N_2O and CH_4 based on the mixed layer depth estimates listed in Table 1.

Groups of individual N_2O profiles show common features that allow them to be conveniently grouped into several "types" coincident with Longhurst (1998) provinces (Fig. 1, Table 1). In contrast, the CH_4 data are not amenable to such analysis; the profiles show far greater similarity in shape and span smaller concentration ranges.

3.1.1. N_2O and Longhurst provinces

Vertical N_2O profiles are shown in Fig. 2. SSTC and NADR were only encountered during AMT12 and CNRY was only encountered during AMT13. All other provinces were sampled during both cruises (Table 1). The N_2O profiles for SSTC and NADR (surface high-latitude south and north Atlantic, respectively) were similar in general shape, being characterized by small increases in concentration with depth between the surface and the base of the mixed layer; overall increases were ~0.5–2 nmol L^{-1} at SSTC, and ~0.3–0.8 nmol L^{-1} at NADR (mixed layer means given in Table 3). Below the mixed layer in both cases N_2O was essentially constant down to ~300 m (SSTC ~13 ± 1.3 nmol L^{-1}, 124 ± 7% saturation; NADR ~8.9 ± 1.3 nmol L^{-1}, 106 ± 13% saturation). For comparison the ranges of N_2O concentrations reported by Walter et al. (2006) for the cold temperate N. Atlantic between 40 and 50°N along 10–50°W (mixed layer, 8.6 ± 1.4 nmol L^{-1}; sub-thermocline 11.3 ± 1.5 nmol L^{-1}) are not significantly different from our data for NADR during AMT12.

The highest mean mixed layer N_2O encountered during AMT was in the CNRY province (Table 3); here the maximum surface N_2O concentration was 9.7 nmol L^{-1} (~150% saturation; 2 m depth, station AMT13_28). Below the CNRY mixed layer N_2O concentrations increased rapidly during AMT13, reaching an approximately constant 30 ± 5 nmol L^{-1} (~370 ± 40% saturation) between 100 and 300 m. Corresponding NO_3^- concentrations generally exceeded 35 μmol L^{-1} (mean 37 ± 2.9 μmol L^{-1}) and O_2 decreased significantly below the mixed layer to a mean ~60 μmol L^{-1} (range 39–78 μmol L^{-1}) below ~70 m depth (data not shown). To our knowledge these vertical profile data are the first to be reported for the Mauritanian upwelling region within the CNRY province. N_2O in the CNRY mixed layer (Table 3) was significantly higher than previously reported values ~113–118% around the southern boundary of CNRY adjacent to the Guinea Shelf between 7 and 12°N (Oudot et al., 2002; Walter et al., 2006). In contrast, Weiss et al. (1992) found 130–140% saturation and Rhee (2000) found 102–115% saturation, in surface waters between 10 and 20°N close to 20°W.

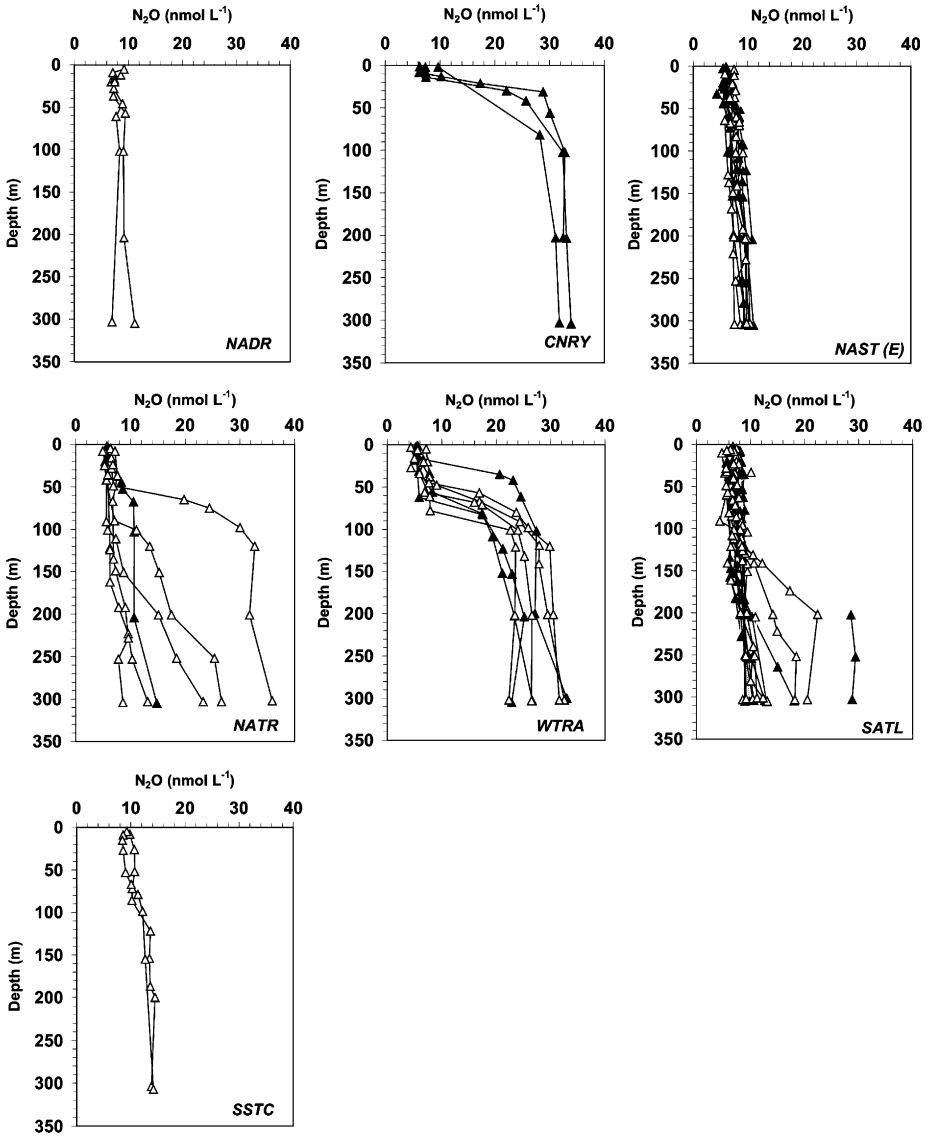

Fig. 2. Vertical profiles of N_2O concentration during AMT12 (clear triangles) and AMT13 (filled triangles) grouped in relation to Longhurst (1998) province.

The SATL is the largest of the provinces encountered during AMT, spanning approximately 36° of latitude. Mean mixed layer N_2O (Table 3) was very close to the ranges found by Weiss et al. (1992), Butler et al. (1995), and Rhee (2000) (~98–108% saturation) during surface surveys in this region. Vertical N_2O profiles south of ~26°S were similar during both cruises, exhibiting a rather mild linear increase in concentration between the surface and 300 m of 0.7–6.8 and 0.9–6.4 nmol L^{-1} for the austral autumn and austral spring, respectively (Fig. 2). These stations showed a weak trend of increasing N_2O at 300 m depth toward lower latitudes. North of 26°S within the SATL N_2O in the upper 150 m was similar to surface levels further south. However, below this depth there was a progressive increase in N_2O concentration toward the northern SATL boundary during both seasons. During the austral autumn N_2O in the deepest sample from AMT12_23 (301 m, Table 1) was 12.3 nmol L^{-1} (149% saturation). Further north (AMT12_29) this reached 22.4 nmol L^{-1} (272% saturation) at 302 m. Similarly, during the austral spring N_2O in the deepest sample from AMT13_53 (304 m, Table 1) was 12.6 nmol L^{-1} (148% saturation) and this increased to 28.8 nmol L^{-1} (295% saturation) at AMT13_44 (302 m) further north. The northward increase in N_2O below ~150 m continued into WTRA; N_2O reached 31.6 nmol L^{-1} (340% saturation) at ~302 m at AMT12_40 and 33 nmol L^{-1} (360% saturation) at ~300 m at AMT13_34. Across the WTRA the concentrations of N_2O were consistently high; ~22–33 nmol L^{-1} (265–360% saturation) during AMT12 and ~21–33 nmol L^{-1} (240–360% saturation) during AMT13. Walter et al. (2006) reported their highest N_2O concentration (37.3 nmol L^{-1} at 400 m depth) adjacent to the Guinea Dome, located approximately equidistant between AMT12_40 and AMT13_34 (Fig. 1) and Oudot et al. (2002) found ~60 nmol L^{-1} at ~400 m in the eastern WTRA. In addition Walter et al. (2006) found shallower N_2O maxima (240–280 m depth) further south towards the equator corresponding to $\sigma_\theta = 26.6$–27.0; this range in σ_θ is identical to that for the N_2O maxima observed in the tropical Atlantic during AMT12 and AMT13. The trend in northerly increasing N_2O at depth also persisted into NATR; 36 nmol N_2O L^{-1} (397% saturation) was recorded at ~302 m at station AMT12_42. However, further north N_2O at depth again began to decrease; the corresponding 300 m concentration at AMT12_51 being only 8.7 nmol L^{-1} (119% saturation). Profiles from NAST(E) were similar during both cruises, being characterized by a mild, approximately linear increase in N_2O with depth from the base of the mixed layer to the deepest sample of ~1.9–3.7 and 3.8–6.7 nmol L^{-1} for

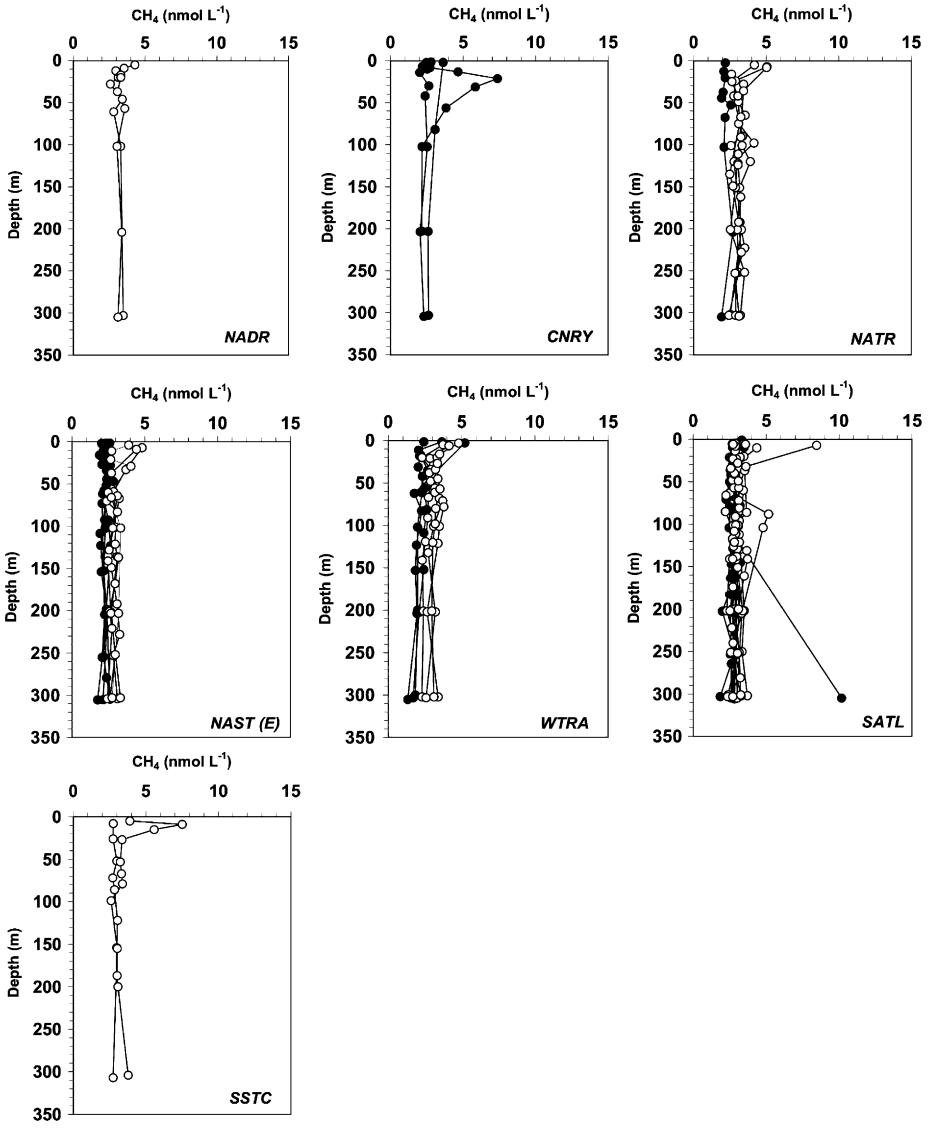

Fig. 3. Vertical profiles of CH_4 concentration during AMT12 (clear triangles) and AMT13 (filled triangles) grouped in relation to Longhurst (1998) province.

AMT12 and AMT13, respectively. The differences between the magnitude of increase in N_2O with depth between AMT12 and AMT13 is most likely a result of spatial variability as the two cruise tracks were significantly different within the NAST(E). In addition some undersaturations of a few percent were observed in some near-surface samples; however, most samples showed supersaturation (Table 3). For comparison Weiss et al. (1992) and Rhee (2000) found saturations close to atmospheric equilibrium with NAST(E).

Generally our mean percent N_2O saturations calculated by Longhurst province for the tropical Atlantic are more variable than those previously reported. The largest variations occur in the WTRA; $109 \pm 21\%$. However, it must be noted that despite the larger variations, the mean for this region is close to mean surface saturations previously reported; ~104–108% saturation (Oudot et al., 2002; Walter et al., 2006).

3.1.2. *Vertical distribution of CH_4*

In contrast to the situation for N_2O, the main features of the observed CH_4 distributions do not clearly correspond to Longhurst provinces. However, in order to facilitate comparisons mean mixed layer concentrations and percent saturations of CH_4 are nevertheless summarized on this basis (Table 3).

The vertical CH_4 profiles are shown in Fig. 3. Within the SAG (~26 to ~6°S) mixed layer CH_4 was rather variable, both within and between the individual cruises; 3.7 ± 1.7 nmol $CH_4\,L^{-1}$ ($201 \pm 98\%$ saturation) for AMT12 and 2.8 ± 0.3 nmol $CH_4\,L^{-1}$ ($155 \pm 17\%$ saturation) for AMT13 displaying considerable seasonal variation and highlights that the SAG is a significant source of CH_4 to the atmosphere. This is also a feature when the mean mixed layer CH_4 concentration is calculated for the SATL province as a whole (Table 3). Previous underway analyses of near-surface SAG waters (sample inlet at 6 m depth) during AMT7 (September–October 1998) ranged from a few % undersaturation to approximately 108% supersaturation (Rhee, 2000). Notwithstanding the fact that the AMT12, AMT13 and AMT7 cruise tracks were somewhat different, AMT7 was more westerly than either AMT12 or AMT13, it is perhaps not surprising that the CH_4 saturations found on AMT7 (Rhee, 2000) were much lower than those from either AMT12 or AMT13. Underway equilibrated CH_4 concentrations are frequently significantly lower than those obtained from CTD samples collected simultaneously from the same depth (Bange, pers. comm.). The discrepancy presumably reflects solubility and response time considerations for CH_4, and appears not to be a problem for N_2O (Bange, pers. comm.).

Below the mixed layer within the SATL province north of 26°S CH_4 saturation decreased toward lower latitudes on both cruises, the opposite of the situation for N_2O. Despite the comparative mixed layer variabilities mean CH_4 at 300 m depth between ~26 and 6°S during AMT12 (2.7 ± 0.4 nmol L^{-1}, range 2.4–3.3 nmol L^{-1}; $119 \pm 20\%$ saturation) and AMT13 (2.5 ± 0.5 nmol L^{-1}, range 1.9–3 nmol L^{-1}; $110 \pm 25\%$ saturation) was not significantly different; in each case the lower ends of the above ranges represent lower latitude stations. The mean CH_4 concentrations at ~300 m between 6°S and 23.5°N were in contrast, significantly different: 2.8 ± 0.4 nmol L^{-1} (range 2.3–3.4 nmol L^{-1}, $121 \pm 19\%$ saturation) during AMT12 (AMT12_33 to AMT12_51) and 1.7 ± 1.3 nmol L^{-1}

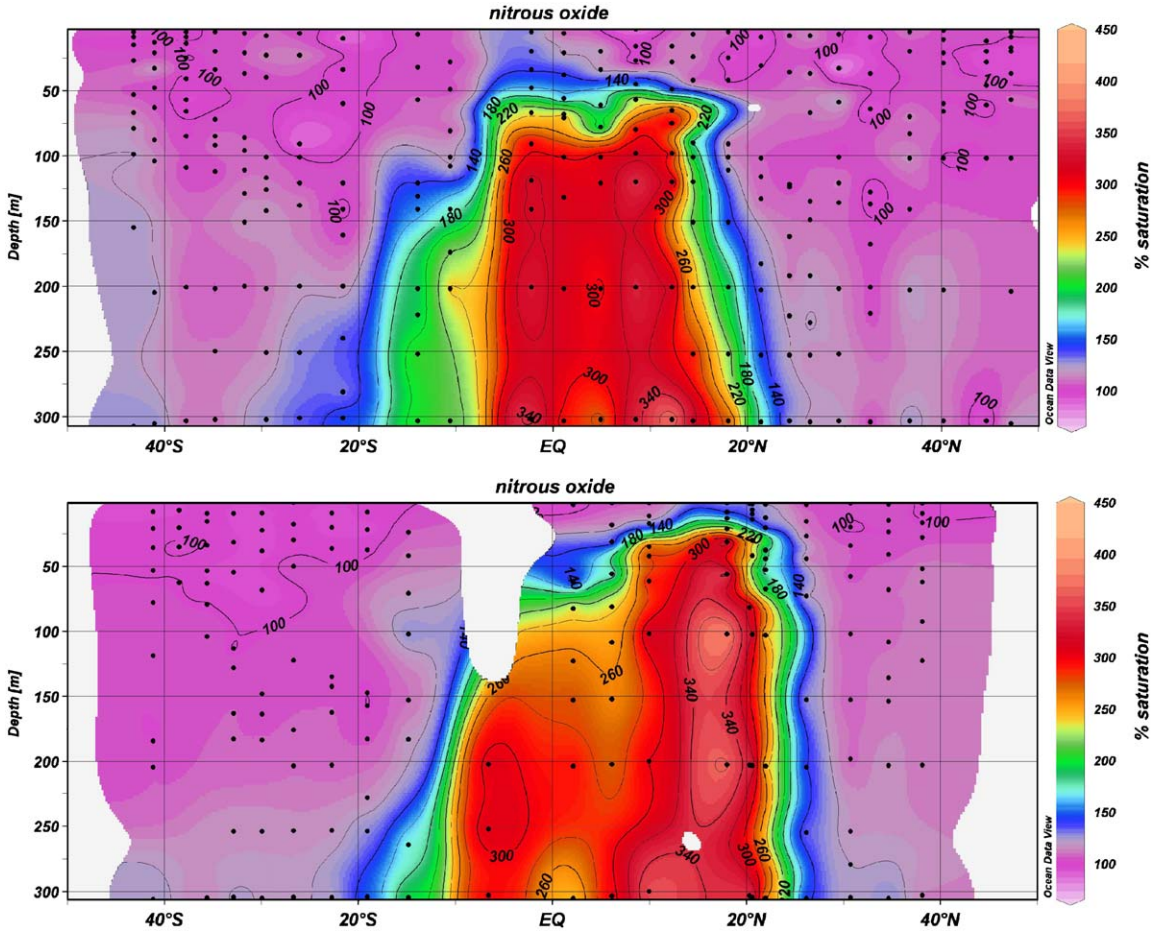

Fig. 4. Latitudinal distributions of N_2O percent saturation in the upper 300 m of the water column during AMT12 (top) and AMT13 (bottom). Black dots represent sampling depths.

(range 1.3–1.9 nmol L^{-1}, 71±14% saturation) during AMT13 (AMT13_24 to AMT13_40). Oudot et al. (2002) similarly, reported CH_4 saturations ~50–90% for a latitudinal transect at 4.30°S. North of 25°N during AMT12 mean mixed layer CH_4 (3.5±0.7 nmol L^{-1}, range 2.6–4.8 nmol L^{-1}; 164±42% saturation) was considerably higher than during AMT13 (2.3±0.2 nmol L^{-1}, range 1.9–2.6 nmol L^{-1}; 120±12% saturation). Similarly, below the mixed layer the boreal spring mean was overall higher than during autumn: AMT12; 3±0.4 nmol L^{-1} (range 2.4–4 nmol L^{-1}, 139±18% saturation), AMT13; 2.3±0.2 nmol L^{-1} (range 1.8–2.9 nmol L^{-1}, 107±13% saturation). The higher mixed layer mean during AMT12 reflects several near surface samples with CH_4 saturations in excess of 200% saturation at stations north of the tropics. Generally previous CH_4 data for the surface waters of the subtropical North Atlantic agree more closely with the data from AMT13 than those from AMT12 with saturation values in the range ~96–150% (e.g. Scranton and Brewer, 1977; Conrad and Seiler, 1988; Seifert et al., 1999; Rhee, 2000) with values generally increasing on the approach towards continental shelf regions.

Tropical Atlantic mixed layer CH_4 was considerably higher in the central region (AMT12: 3.7±0.8 nmol L^{-1}, 183±43% saturation) than further east (AMT13: 2.3±0.5 nmol L^{-1}, 128±26% saturation). The mean CH_4 saturations in eastern tropical Atlantic mixed layer during AMT13 agree closely with previously reported values for tropical Atlantic open ocean studies; ~100–140% (Conrad and Seiler, 1988; Rhee, 2000; Oudot et al., 2002). Previously Conrad and Seiler (1988) reported CH_4 concentrations ~50–93 nL L^{-1} for the upper 20 m of the tropical Atlantic between 3°N and 2°S along the 22°W. These data translate to approximate CH_4 saturations ~130–250% in the uppermost 4 m and ~140–220% at 20 m depth; Moreover, Oudot et al. (2002) report ~220% CH_4 saturations measured in surface waters around 4°W, 4.30°S. The mean mixed layer CH_4 saturations reported here for the Central Tropical Atlantic (183±43%) are among the highest values thus far reported. Our data confirm the Central Atlantic Ocean as a potentially significant source of atmospheric CH_4.

3.1.3. *Latitudinal-depth contrast in N_2O and CH_4*

The latitudinal-depth distributions of N_2O and CH_4 saturation were strikingly different from each other and broadly persistent across the two seasons (Figs. 4 and 5). The most striking feature of both the AMT12 and AMT13 N_2O distributions (Fig. 4) may best be described as a very well-defined "plume" of exceptionally high supersaturations ~140–340% N_2O located between about 23.5°S and 23.5°N, extending from 20 to 50 m below the surface to below the deepest waters sampled, and broadly coincident with the lowest observed values of CH_4 saturation (Fig. 5). The same feature is readily discernable in corresponding salinity and temperature data (Robinson et al., 2006), and can also be clearly seen in the BLASTII N_2O data set presented in Nevison et al. (2003). Outside the plume N_2O was everywhere at, or very close to, atmospheric equilibrium. Outside the regions of comparatively low CH_4 saturation associated with the N_2O plumes, CH_4 was essentially everywhere quite strongly supersaturated. To what extent the plume suppresses the CH_4 signal in the near-surface

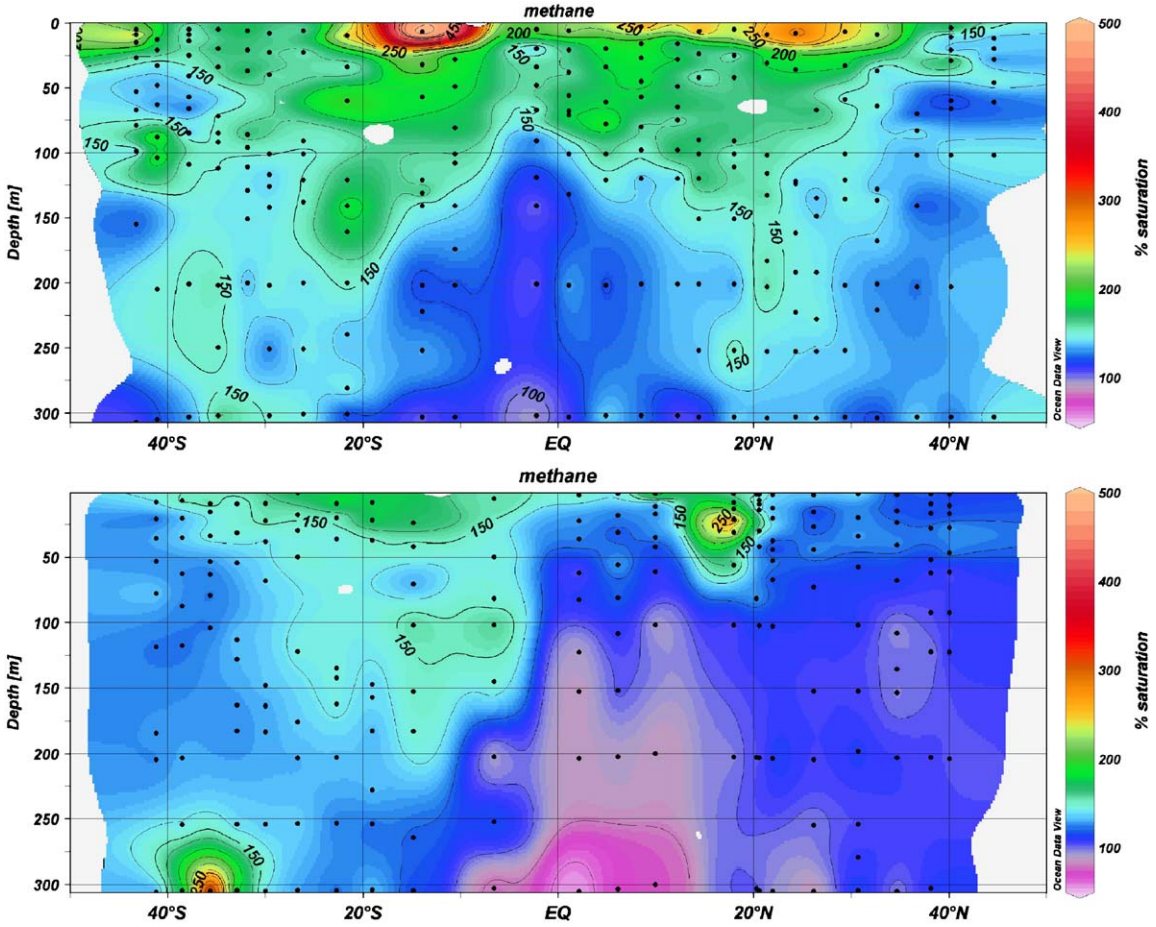

Fig. 5. Latitudinal distributions of CH_4 percent saturation in the upper 300 m of the water column during AMT12 (top) and AMT13 (bottom). Black dots represent sampling depths.

waters above it remains unclear, however, higher near-surface CH_4 encountered outside the plume implies some degree of mixing with waters above 20–50 m. Indeed a major CH_4 feature during AMT12 was a surface region ~25 m deep between ~25°S and 35°N (i.e. outside the "plume") in which CH_4 saturation exceeded 200% and with two localized maxima around 15–20°S and 20–30°N, each with >250% CH_4 saturation. This feature was much weaker during AMT13; only a sub-surface region of exceptionally high CH_4 saturation was discernable, centred at ~25 m depth around 16°N. Oudot et al. (2002) observed CH_4 undersaturation and N_2O supersaturation coincident at about 400 m depth in the eastern and western basins of the tropical Atlantic around 5°S, accompanying a well-documented O_2 minimum (Reid, 1989). It seems likely that this is part of the feature identified in Figs. 4 and 5.

The contrasting distributions of N_2O and CH_4 in the upper 300 m of the Atlantic water column reflect the relative sources and sinks of these two gases in oceanic waters, coupled with upward transport.

3.2. Source of the upwelled N_2O

Further insight into the production mechanisms of N_2O in the subsurface ocean may be derived by examining the relationships between ΔN_2O and AOU (Yoshinari, 1976; Suntharalingam and Sarmiento, 2000; Nevison et al., 2003) and between ΔN_2O and NO_3^- (Cohen and Gordon, 1979; Walter et al., 2006), where ΔN_2O is the difference between N_2O measured *in situ* and its theoretical concentration equivalent to 100% saturation. It is generally agreed that a strong positive correlation between these variables is evidence for nitrification as the main source of N_2O (e.g. Yoshinari, 1976; Elkins et al., 1978; Cohen and Gordon, 1979; De Wilde and Helder, 1997; Patra et al., 1999; Oudot et al., 2002; Nevison et al., 2003; Walter et al., 2006). The relationships between ΔN_2O and AOU vary considerably between different ocean regions and as a function of depth (e.g. Yoshinari, 1976; Elkins et al., 1978; Cohen and Gordon, 1979; Butler et al., 1989; Law and Owens, 1990; Oudot et al., 2002; Nevison et al., 2003; Walter et al., 2006) and may reflect the sensitivity of nitrifiers to varying ambient O_2 (e.g. Goreau et al., 1980; Poth and Focht, 1985). For example De Wilde and Helder (1997) found a significant increase in N_2O at O_2 concentrations below 15–20 μmol L^{-1} in the Somali Basin.

We investigated the mechanism of N_2O production within the tropical Atlantic by examining the relationships between ΔN_2O and AOU and between ΔN_2O and NO_3^- for sub-mixed layer waters during AMT12 and AMT13 (Fig. 6). For the tropical Atlantic, i.e. the region between 23.5°S and 23.5°N, strong correlations between ΔN_2O and AOU (AMT12: $r^2 = 0.82$, $n = 36$, $p \leqslant 0.001$; AMT13: $r^2 = 0.85$, $n = 29$, $p \leqslant 0.001$) and between ΔN_2O and NO_3^- (AMT12: $r^2 = 0.86$, $n = 36$, $p \leqslant 0.001$; AMT13: $r^2 = 0.68$, $n = 29$, $p < 0.001$) suggest a nitrification source for the upwelled N_2O in agreement with previous studies in the tropical Atlantic (e.g. Oudot et al., 2002; Walter et al., 2006). The relationship between ΔN_2O and AOU within the tropical Atlantic is remarkably similar for both its central (AMT12) (1) and eastern sectors (AMT13) (2):

$$\Delta N_2O = 1.135 + 0.121AOU \quad (1)$$

$$\Delta N_2O = 1.047 + 0.106AOU \quad (2)$$

This similarity implies a common N_2O source across much of the tropical Atlantic Ocean. In contrast, Walter et al. (2006) report a somewhat different relationship for tropical Atlantic water above 500 m ($> \sigma_\theta = 27.1$):

$$\Delta N_2O = 2.4381 + 0.0785AOU \quad (3)$$

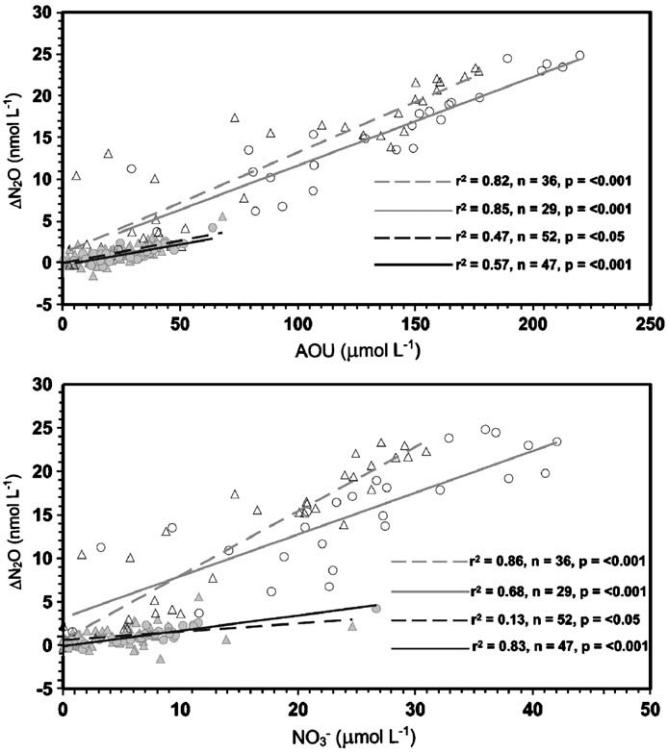

Fig. 6. Relationship between ΔN_2O and AOU (top) and for ΔN_2O and NO_3^- (bottom); AMT12 between 23.5°S and 23.5°N (empty triangles and grey dashed line) and south of 23.5°S and north of 23.5°N (filled triangles and black dashed line); AMT13 between 23.5°S and 23.5°N (empty circles and grey solid line) and south of 23.5°S and north of 23.5°N (filled circles and black solid line).

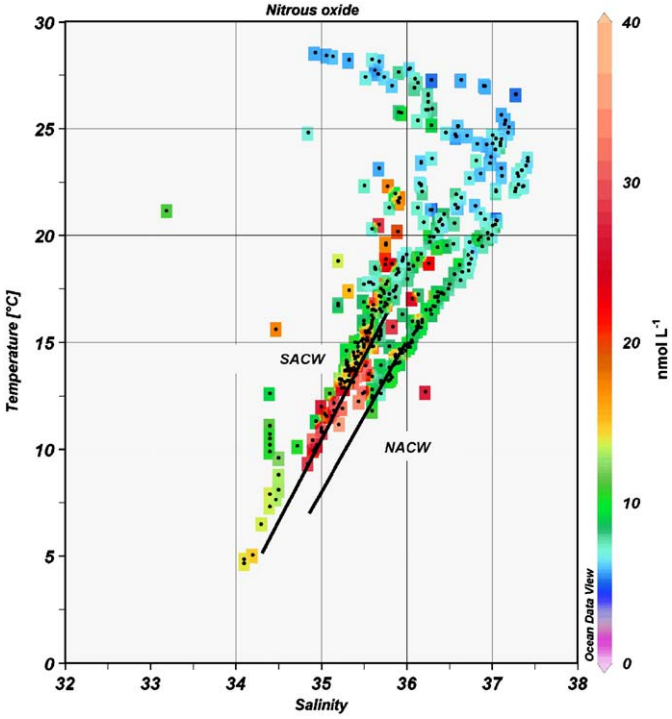

Fig. 7. Relationship between salinity, temperature and N_2O during AMT.

The discrepancy between the AMT ΔN_2O:AOU relationships and those of Walter et al. (2006) is likely related to the different depths over which these relationships were derived.

During AMT highest N_2O in the tropical Atlantic was associated with σ_θ values consistent with South Atlantic Central Water (SACW) (e.g. Emery and Meincke, 1986; Poole and Tomczak, 1999) (Fig. 7) and the majority of highest N_2O concentrations are associated with $\sigma_\theta = 26.6–27.4$, suggesting that the N_2O may be produced predominantly in this water mass. Similarly, Walter et al. (2006) found highest N_2O concentrations in the eastern basin within SACW; 37.3 nmol L^{-1}, which prompted them to suggest nitrification as the primary N_2O production mechanism in the tropical Atlantic. Due to the similarity of our tropical Atlantic ΔN_2O:AOU relationships for AMT12 (central basin) and AMT13 (eastern basin) we propose that the elevated N_2O in these regions (Fig. 7) is primarily a consequence of nitrification within the SACW.

3.3. Source of CH_4 in the mixed layer

Within the well-oxygenated ocean surface mixed layer, CH_4 supersaturations are a common feature (e.g. Lamontagne et al., 1973; Scranton and Brewer, 1977; Scranton and Farrington, 1977; Owens et al., 1991; Patra et al., 1998) and have been ascribed to methanogenesis by O_2-tolerant methanogens inside anoxic "microniches" maintained by bacterial activity (Oremland, 1979). This view is supported by the isolation of an "oxic" methanogen from coastal waters (Cynar and Yayanos, 1991) and the identification of methanogens in marine zooplankton guts and particles (Marty et al., 1997). Although some studies have reported close associations between CH_4 and indicators of primary productivity such as chlorophyll-a (e.g. Conrad and Seiler, 1988; Oudot et al., 2002), other studies have found either only weak correlations or no correlation at all (e.g. Upstill-Goddard et al., 1999; Holmes et al., 2000), and we found no such correlation during either AMT12 or AMT13, which qualitatively tends to favour the "anoxic microniche" hypothesis. Although total suspended particle concentrations with which to directly test this were unavailable during AMT, particulate organic carbon and nitrogen (POC and PON) were measured. However, we found no significant relationships between CH_4 and either POC or PON (Forster, 2006). Similarly, although Traganza et al. (1979) report a correlation between CH_4 and zooplankton ATP, during AMT neither zooplankton numbers or biomass (San Martin et al., 2006) showed any clear correlation with CH_4 (Forster, 2006).

The regions of low CH_4 within the plume reflect upwelling of deep water in which CH_4 is depleted by bacterial oxidation (e.g. Ward and Kilpatrick, 1993; Ward et al., 1987).

3.4. Sea-to-air emissions fluxes

Sea-to-air emission flux densities (F, mol m^{-2} d^{-1}) of N_2O and CH_4 at individual stations were estimated from their measured partial pressures in seawater and air, using

$$F = k_w L \Delta p,$$

where k_w is the gas transfer velocity for N_2O or CH_4 (cm h^{-1}), L is the appropriate gas solubility (mol cm^{-3} atm^{-1}) at ambient temperature and salinity, and Δp is the gas partial pressure difference (natm.) across the sea–air interface. The empirical relationships of Liss and Merlivat (1986) and Wanninkhof (1992) were used to quantify the wind speed dependence of k_w; we derived k_w for N_2O and CH_4 from the corresponding values for CO_2 using appropriate Schmidt numbers, Sc (Wanninkhof, 1992). For Liss and Merlivat (1986), k_w for CO_2 was multiplied by $(Sc/600)^n$ ($n = -0.67$ for $U_{10} < 3.6$ m s^{-1}, $n = -0.5$ for $U_{10} > 3.6$ m s^{-1}, U_{10} is the 10 m wind speed). For Wanninkhof (1992), k_w was multiplied by $(Sc/660)^{-0.5}$. Alternative wind speed related parameterizations of k_w (e.g. Erickson, 1993; Nightingale et al., 2000) yield air–sea fluxes that are intermediate between these values; hence using the relationships of Liss and Merlivat (1986) and Wanninkhof (1992) provides upper and lower boundaries to our flux estimates. In situ wind speeds were recorded at 60 s intervals using an anemometer located on the ship's foremast ~22 m above sea level. These were subsequently corrected for ship speed and course, and lateral flow distortion (Yelland et al., 1998), and converted to U_{10}^n, the equivalent wind speed at 10 m above the sea surface for neutral atmospheric stability, as described in Nightingale et al. (2000). Wind speeds used in estimating individual station fluxes are the means of values recorded within 0.050° of the station to allow for off-station drift during sampling. Values of Δp for N_2O and CH_4 are mean values determined over the mixed layer depths (Table 1).

Fig. 7 shows the individual station N_2O and CH_4 emission flux densities (μmol m^{-2} d^{-1}) and the corresponding mean mixed layer partial pressures (natm) as functions of latitude. Both gases showed a high degree of inter-station flux variability. The overall ranges of variability were two orders of magnitude for N_2O and two to three orders of magnitude for CH_4; these ranges primarily reflect large differences in ambient wind speeds between stations rather than variability in mixed layer gas inventories (Fig. 7).

Mean flux densities derived from the individual station fluxes for each Longhurst province, and the corresponding province-based emissions fluxes (Tg N_2O or CH_4 yr^{-1}) are summarized in

Table 4
Mean flux densities and total emissions of N_2O and CH_4 grouped according to Longhurst province during AMT12 and AMT13.

Province	Surface area ($\times 10^6$ km^2)	AMT12 Average flux density (μmol m^{-2} d^{-1})		AMT13 Average flux density (μmol m^{-2} d^{-1})		Annual flux (Tg yr^{-1})	
		N_2O	CH_4	N_2O	CH_4	N_2O	CH_4
SSTC	4.1	0.79–1.57	3.88–6.81	n.s.	n.s.	0.05–0.10[a]	0.09–0.16[a]
SATL	17.8	0.97–1.62	3.63–5.89	0.25–0.41	3.16–5.64	0.17–0.29	0.35–0.59
WTRA	5.4	1.17–2.13	3.92–6.43	0.16–0.33	1.96–3.43	0.06–0.11	0.09–0.16
NATR	8.3	0.60–0.87	6.14–9.69	−0.02 to −0.04	3.13–5.93	0.04–0.06	0.22–0.40
NAST(E)	4.4	0.72–1.05	1.91–3.65	0.36–0.71	1.21–2.26	0.04–0.06	0.04–0.08
NADR	3.5	−0.04 to −0.08	0.46–0.90	n.s.	n.s.	−0.002 to −0.004[a]	0.01–0.02[a]
CNRY	0.8	n.s.	n.s.	2.73–4.65	2.31–4.04	0.04–0.06[b]	0.01–0.02[b]
Total	44.3					0.40–0.68	0.81–1.43

Upper and lower limits are representative of fluxes and emissions calculated using the models of Liss and Merlivat (1986) and Wanninkhof (1992), respectively.
n.s. refers to not sampled.
[a] Annual flux calculated from samples collected during austral fall.
[b] Annual flux calculated from samples collected during boreal fall.

Table 4. In each case the lower and higher figures in each range refer to estimates deriving from the k_w–wind speed relationships of Liss and Merlivat (1986) and Wanninkhof (1992), respectively. Although, we have previously summarized a subset of these data (Robinson et al., 2006), we below present the first complete summary analysis of the full AMT data set for N_2O and CH_4 emissions.

Due to differences in the northern hemisphere cruise tracks between the two cruises only the emissions fluxes from SATL are amenable to a seasonal comparison. This province had the highest emissions fluxes for both gases, principally as a consequence of its comparatively large surface area (~40% of the total, Table 4) rather than as a consequence of high individual flux densities. Interestingly, although SATL N_2O emissions were around 4 times higher during AMT12 than during AMT13, there was no comparable seasonality in CH_4 emissions; the difference for N_2O cannot therefore be explained in terms of the ambient wind speed distributions. Rather, mixed layer N_2O showed comparatively high inter-station variability during AMT12 (Fig. 7), causing a bias towards higher emissions values. To the best of our knowledge our N_2O and CH_4 emissions flux estimates for SATL (Table 4) are the only such estimates reported for this large Atlantic province (Fig. 8).

CNRY had exceptionally high individual station flux densities for N_2O but due to its comparatively small surface area its contribution to the total Atlantic N_2O flux is rather small (Table 4). Previously Nevison et al. (2004) estimated a total atmospheric N_2O source due to coastal upwelling globally $\sim 0.31 \pm 0.2\ \mathrm{Tg\ yr^{-1}}$.

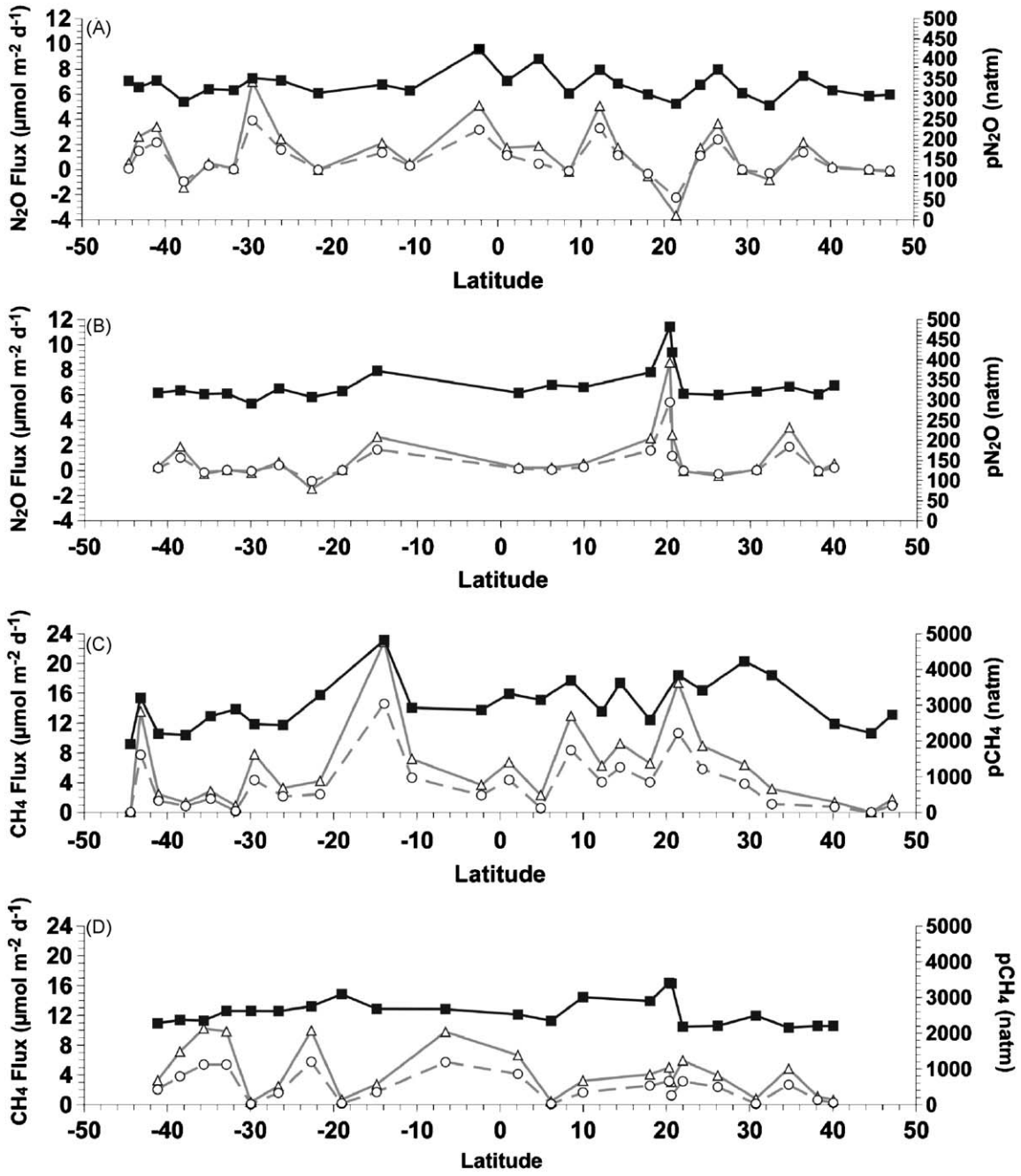

Fig. 8. Estimated sea–air flux of N_2O for stations sampled during AMT12 (A) and AMT13 (B) and for CH_4 during AMT12 (C) and AMT13 (D). Fluxes are estimated using the models of Liss and Merlivat (1986) (empty circles and grey dashed line) and Wanninkhof (1992) (empty triangles and solid grey line). The average partial pressure in the mixed layer at each station is shown by the black filled squares and black solid line).

Adjusting for the larger surface area of CNRY relative to the area of East African upwelling defined by Nevison et al. (2004), our estimate for CNRY is, on a unit area basis; in good agreement with the Nevison et al. (2004) estimate. We can conclude that CNRY represents an approximately average N_2O source strength as compared to other regions experiencing significant upwelling. However, for CH_4 CNRY appears to be a comparatively weak source. NADR appears to be a similarly weak CH_4 source but it is approximately neutral or a very weak sink with respect to N_2O (Table 4). For WTRA our emissions estimates show good agreement with those derived both by Oudot et al. (2002) and Walter et al. (2004).

Considering the large sizes of the individual Longhurst provinces (Table 4) and our restriction to an essentially two-dimensional transect on each cruise, our emissions flux estimates deriving from these are, as with other studies, subject to uncertainties arising from the fact that our ability to account for within-province spatial variability, and to a lesser extent temporal variability, was necessarily limited. Clearly such uncertainties are rather difficult to evaluate without additional data. Importantly, however, our mixed layer concentration means for both N_2O and CH_4 are in fact rather close to values found in previous work at other locations in these areas. This gives us confidence in our resulting sea-to-air emissions flux estimates.

The Longhurst provinces detailed in Table 4 together make up ~42% of the total surface area of the Atlantic Ocean, rendering our data the most extensive contiguous surveys of both N_2O and CH_4 for this ocean basin. An earlier estimate for the total oceanic CH_4 emission of $0.4\,Tg\,yr^{-1}$ (Bates et al., 1996) was derived from latitudinal transects of the open-ocean Pacific, and so is similar in this respect to the AMT cruise tracks in that it involved minimal sampling of coastal and/or shelf waters. Nevertheless our total estimate for 42% of the Atlantic Ocean exceeds this (Table 4), bringing into question the validity of this previous global estimate for CH_4. More recent estimates of total marine source strengths are, for N_2O, $4.71–6.28\,Tg\,yr^{-1}$ (Mosier et al., 1998; Kroeze et al., 1999; Nevison et al., 1995), and for CH_4 $11–18\,Tg\,yr^{-1}$ (Bange et al., 1994; Lelieveld et al., 1998). Based on these estimates our data imply that the Atlantic Ocean might account for ~6–15% and 4–13%, respectively, of the total marine sources of atmospheric N_2O and CH_4. Bange et al. (1994) derived an estimate of the total Atlantic CH_4 emission $\sim 0.9–1.4\,Tg\,yr^{-1}$; this is close to our estimate for 42% of the Atlantic Ocean. Based on our data and making the assumption that our flux estimates are indeed representative of the whole Atlantic, this ocean basin could be a 2-fold larger atmospheric CH_4 source than previously thought. However, testing this assumption and further refining our flux estimates will require initiating a more detailed sampling strategy both spatially and seasonally, than was possible during AMT. Notwithstanding the uncertainties in our data set, given that the Atlantic Ocean accounts for around 20% of the global ocean surface, on a unit area basis it appears that the Atlantic may be a slightly weaker source of atmospheric N_2O than other open ocean regions but it could make a somewhat larger contribution to marine-derived atmospheric CH_4 than previously thought.

Acknowledgments

Numerous colleagues assisted us in many ways during AMT and without them this study would not have been realized. In particular we recognize the sterling efforts of the captains and crews of RRS. James Clark Ross and the Principal Scientists Tim Jickells and Carol Robinson on AMT12 and AMT13, support given to us by staff from the UK Natural Environment Research Council (NERC), in particular UK Oceanographic Research Services (UKORS) and Research Ships Unit (RSU), the British Antarctic Survey (BAS), and all those AMT scientists whom we have failed to include here. This work was supported by NERC through an award (NER/O/S/2001/00680) made to the Atlantic Meridional Transect Consortium. This is contribution number 170 of the AMT programme.

References

Bange, H.W., 2006. New directions: the importance of oceanic nitrous oxide emissions. Atmospheric Environment 40, 198–199.
Bange, H.W., Bartell, U.H., Rapsomanikis, S., Andreae, M.O., 1994. Methane in the Baltic and North Seas and a reassessment of the marine emissions of methane. Global Biogeochemical Cycles 8 (4), 465–480.
Bange, H.W., Rapsomanikis, S., Andrae, M.O., 1996. Nitrous oxide in coastal waters. Global Biogeochemical Cycles 10 (1), 197–207.
Bates, T.S., Kelly, K.C., Johnson, J.E., Gammon, R.H., 1996. A re-evaluation of the open ocean source of methane to the atmosphere. Journal of Geophysical Research—Atmospheres 101 (D3), 6953–6961.
Benson, B.B., Krause, D., 1984. The concentration and isotopic fractionation of oxygen dissolved in fresh-water and seawater in equilibrium with the atmosphere. Limnology and Oceanography 29 (3), 620–632.
Brewer, P.G., Riley, J.P., 1965. The automatic determination of nitrate in seawater. Deep-Sea Research 12, 765–772.
Butler, J.H., Elkins, J.W., Thompson, T.M., Egan, K.B., 1989. Tropospheric and dissolved N_2O of the West Pacific and East-Indian Oceans during the El-Nino Southern Oscillation event of 1987. Journal of Geophysical Research—Atmospheres 94 (D12), 14865–14877.
Butler, J.H., Lobert, J.M., Yvon, S.A., Geller, L.S., 1995. The distribution and cycling of halogenated trace gases. In: Kattner, G., Fütterer, D.K. (Eds.), Reports on Polar Research No. 168-The expedition ANTARKTIS XII of RV "Polarstern" in 1994/95: Reports of legs ANT XII/1 and 2. Alfred Wegener Institute for Polar and Marine Research, Bremerhaven. pp. 33–40.
Cohen, Y., Gordon, L.I., 1979. Nitrous-oxide production in the ocean. Journal of Geophysical Research—Oceans and Atmospheres 84 (NC1), 347–353.
Conrad, R., Seiler, W., 1988. Methane and hydrogen in seawater (Atlantic Ocean). Deep-Sea Research I 35 (12), 1903–1917.
Crutzen, P.J., 1991. Methane's sinks and sources. Nature 350 (6317), 380–381.
Cynar, F.J., Yayanos, A.A., 1991. Enrichment and characterization of a methanogenic bacterium from the oxic upper layer of the ocean. Current Microbiology 23 (2), 89–96.
De Wilde, H.P.J., Helder, W., 1997. Nitrous oxide in the Somali Basin: the role of upwelling. Deep-Sea Research II 44 (6–7), 1319–1340.
Dlugokencky, E.J., Masarie, K.A., Lang, P.M., Tans, P.P., 1998. Continuing decline in the growth rate of the atmospheric methane burden. Nature 393 (6684), 447–450.
Dlugokencky, E.J., Walter, B.P., Masarie, K.A., Lang, P.M., Kasischke, E.S., 2001. Measurements of an anomalous global methane increase during 1998. Geophysical Research Letters 28 (3), 499–502.
Elkins, J.W., Wofsy, S.C., McElroy, M.B., Kolb, C.E., Kaplan, W.A., 1978. Aquatic sources and sinks for nitrous-oxide. Nature 275 (5681), 602–606.
Emery, W.J., Meincke, J., 1986. Global water masses: summary and review. Oceanologica Acta 9, 383–391.
Erickson, D.J., 1993. A stability dependent theory for air–sea gas-exchange. Journal of Geophysical Research—Oceans 98 (C5), 8471–8488.
Forster, G., 2006. Nitrous oxide and methane in the Atlantic Ocean: transects from 52°S to 50°N during AMT. Ph.D. Thesis, University of Newcastle upon Tyne.
Goreau, T.J., Kaplan, W.A., Wofsy, S.C., McElroy, M.B., Valois, F.W., Watson, S.W., 1980. Production of NO_2^- and N_2O by nitrifying bacteria at reduced concentrations of oxygen. Applied Environmental Microbiology 40 (3), 526–532.
Holmes, M.E., Sansone, F.J., Rust, T.M., 2000. Methane production, consumption, and air–sea exchange in the open ocean: an evaluation based on carbon isotopic ratios. Global Biogeochemical Cycles 14, 1–10.
Hooker, S.B., Rees, N.W., Aiken, J., 2000. An objective methodology for identifying oceanic provinces. Progress in Oceanography 45 (3–4), 313–338.
IPCC, 2001. (Houghton, J.T., Ding, Y., Griggs, D.J., Noguer, M., van der Linden, P.J., Dai, X., Maskell, K., Johnson, C.A. (Eds.)), Climate Change 2001: The Scientific Basis. Contribution of Working Group I to the Third Assessment Report of the Intergovernmental Panel on Climate Change. Cambridge University Press, Cambridge, UK, 881pp.
Khalil, M.A.K., Rasmussen, R.A., 1992. The global sources of nitrous-oxide. Journal of Geophysical Research—Atmospheres 97 (D13), 14651–14660.
Kroeze, C., Mosier, A., Bouwman, L., 1999. Closing the global N_2O budget: a retrospective analysis 1500–1994. Global Biogeochemical Cycles 13 (1), 1–8.
Lamontagne, R.A., Swinnerton, J.W., Linnenbom, V.J., Smith, W.D., 1973. Methane concentrations in various marine environments. Journal of Geophysical Research 78 (24), 5317–5324.
Law, C.S., Owens, N.J.P., 1990. Denitrification and nitrous-oxide in the North Sea. Netherlands Journal of Sea Research 25 (1–2), 65–74.
Lelieveld, J., Crutzen, P.J., Dentener, F.J., 1998. Changing concentration, lifetime and climate forcing of atmospheric methane. Tellus Series B—Chemical and Physical Meteorology 50 (2), 128–150.

Liss, P.S., Merlivat, L., 1986. Air–sea gas exchange rates: introduction and synthesis. In: Buat-Ménard, P. (Ed.), The Role of Air–Sea Exchange in Geochemical Cycling. Reidel, Hingham, MA, pp. 113–129.
Longhurst, A., 1998. Ecological Geography of the Sea. Academic Press, New York, 398pp.
Marty, D., Nival, P., Yoon, W.D., 1997. Methanoarchaea associated with sinking particles and zooplankton collected in the Northeastern tropical Atlantic. Oceanologica Acta 20 (6), 863–869.
Morell, J.M., Capella, J., Mercado, A., Bauza, J., Corredor, J.E., 2001. Nitrous oxide fluxes in Caribbean and tropical Atlantic waters: evidence for near surface production. Marine Chemistry 74 (2–3), 131–143.
Mosier, A., Kroeze, C., Nevison, C., Oenema, O., Seitzinger, S., van Cleemput, O., 1998. Closing the global N_2O budget: nitrous oxide emissions through the agricultural nitrogen cycle—OECD/IPCC/IEA phase II development of IPCC Guidelines For National Greenhouse Gas Inventory Methodology. Nutrient Cycling in Agroecosystems 52 (2–3), 225–248.
Nevison, C., Holland, E., 1997. A re-examination of the impact of anthropogenically fixed nitrogen on atmospheric N_2O and the stratospheric O_3 layer. Journal of Geophysical Research—Atmospheres 102 (D21), 25519–25536.
Nevison, C.D., Weiss, R.F., Erickson, D.J., 1995. Global oceanic emissions of nitrous-oxide. Journal of Geophysical Research—Oceans 100 (C8), 15809–15820.
Nevison, C., Butler, J.H., Elkins, J.W., 2003. Global distribution of N_2O and the ΔN_2O-AOU yield in the subsurface ocean. Global Biogeochemical Cycles 17 (4) Art: 1119.
Nevison, C.D., Lueker, T.J., Weiss, R.F., 2004. Quantifying the nitrous oxide source from coastal upwelling. Global Biogeochemical Cycles 18 (1) Art: GB1018.
Nightingale, P.D., Malin, G., Law, C.S., Watson, A.J., Liss, P.S., Liddicoat, M.I., Boutin, J., Upstill-Goddard, R.C., 2000. In situ evaluation of air–sea gas exchange parameterizations using novel conservative and volatile tracers. Global Biogeochemical Cycles 14 (1), 373–387.
Oremland, R.S., 1979. Methanogenic activity in plankton samples and fish intestines—mechanism for *in situ* methanogenesis in oceanic surface waters. Limnology and Oceanography 24 (6), 1136–1141.
Oudot, C., Andrie, C., Montel, Y., 1990. Nitrous-oxide production in the tropical Atlantic-Ocean. Deep-Sea Research I 37 (2), 183–202.
Oudot, C., Jean-Baptiste, P., Fourre, E., Mormiche, C., Guevel, M., Ternon, J.F., Le Corre, P., 2002. Transatlantic equatorial distribution of nitrous oxide and methane. Deep-Sea Research I 49 (7), 1175–1193.
Owens, N.J.P., Law, C.S., Mantoura, R.F.C., Burkill, P.H., Llewellyn, C.A., 1991. Methane flux to the atmosphere from the Arabian Sea. Nature 354 (6351), 293–296.
Patra, P.K., Lal, S., Venkataramani, S., Gauns, M., Sarma, V., 1998. Seasonal variability in distribution and fluxes of methane in the Arabian Sea. Journal of Geophysical Research—Oceans 103 (C1), 1167–1176.
Patra, P.K., Lal, S., Venkataramani, S., de Sousa, S.N., Sarma, V.V.S.S., Sardesai, S., 1999. Seasonal and spatial variability in N_2O distribution in the Arabian Sea. Deep-Sea Research I 46 (3), 529–543.
Poole, R., Tomczak, M., 1999. Optimum multiparameter analysis of the water mass structure in the Atlantic Ocean thermocline. Deep-Sea Research I 46, 1895–1921.
Poth, M., Focht, D.D., 1985. ^{15}N kinetic analysis of N_2O production by *Nitrosomonas europaea*—an examination of nitrifier denitrification. Applied Environmental Microbiology 49 (5), 1134–1141.
Prinn, R., Cunnold, D., Rasmussen, R., Simmonds, P., Alyea, F., Crawford, A., Fraser, P., Rosen, R., 1990. Atmospheric emissions and trends of nitrous-oxide deduced from 10 years of Ale-Gauge data. Journal of Geophysical Research—Atmospheres 95 (D11), 18369–18385.
Reid, J.L., 1989. On the total geostrophic circulation of the south-Atlantic Ocean-flow patterns, tracers, and transports. Progress in Oceanography 23 (3), 149–244.
Rhee, T.S., 2000. The process of air–water gas exchange and its application. Ph.D. Thesis, Texas A&M University.
Robinson, C., Poulton, A.J., Holligan, P.M., Baker, A.R., Forster, G., Gist, N., Jickells, T.D., Malin, G., Upstill-Goddard, R., Williams, R.G., Woodward, E.M.S., Zubkov, M.V., 2006. The Atlantic Meridional Transect (AMT) programme: a contextual view 1995–2005. Deep-Sea Research II 53 (14–16), 1485–1515.
San Martin, E., Harris, R.P., Irigoien, X., 2006. Latitudinal variation in plankton size spectra along the Atlantic Ocean. Deep-Sea Research II 53 (14–16), 1560–1572.
Scranton, M.I., Brewer, P.G., 1977. Occurrence of methane in near-surface waters of western subtropical North-Atlantic. Deep-Sea Research 24 (2), 127–138.
Scranton, M.I., Farrington, J.W., 1977. Methane production in waters off Walvis Bay. Journal of Geophysical Research—Oceans and Atmospheres 82 (31), 4947–4953.
Seifert, R., Delling, N., Richnow, H.H., Kempe, S., Hefter, J., Michaelis, W., 1999. Ethylene and methane in the upper water column of the subtropical Atlantic. Biogeochemistry 44, 73–91.
Suntharalingam, P., Sarmiento, J.L., 2000. Factors governing the oceanic nitrous oxide distribution: simulations with an ocean general circulation model. Global Biogeochemical Cycles 14 (1), 429–454.
Traganza, E.D., Swinnerton, J.W., Cheek, C.H., 1979. Methane supersaturation and ATP-zooplankton blooms in near-surface waters of the Western Mediterranean and the subtropical North Atlantic Ocean. Deep-Sea Research 26A, 1237–1245.
Upstill-Goddard, R.C., Watson, A.J., Liss, P.S., Liddicoat, M.I., 1990. Gas transfer velocities in lakes measure with sulphur hexafluoride. Tellus B—Chemical and Physical Meteorology 42, 364–377.
Upstill-Goddard, R.C., Rees, A.P., Owens, N.J.P., 1996. Simultaneous high-precision measurements of methane and nitrous oxide in water and seawater by single phase equilibration gas chromatography. Deep-Sea Research I 43 (10), 1669–1682.
Upstill-Goddard, R.C., Barnes, J., Owens, N.J.P., 1999. Nitrous oxide and methane during the 1994 SW monsoon in the Arabian Sea/northwestern Indian Ocean. Journal of Geophysical Research—Oceans 104 (C12), 30067–30084.
Walter, S., Bange, H.W., Wallace, D.W.R., 2004. Nitrous oxide in the surface layer of the tropical North Atlantic Ocean along a west to east transect. Geophysical Research Letters 31 (23) Art: L23S07.
Walter, S., Bange, H.W., Breitenbach, U., Wallace, D.W.R., 2006. Nitrous oxide in the North Atlantic Ocean. Biogeosciences 3, 607–619.
Wanninkhof, R., 1992. Relationship between wind-speed and gas-exchange over the ocean. Journal of Geophysical Research—Oceans 97 (C5), 7373–7382.
Ward, B.B., Kilpatrick, K.A., 1993. Methane oxidation associated with mid-depth methane maxima in the Southern California Bight. Continental Shelf Research 13 (10), 1111–1122.
Ward, B.B., Kilpatrick, K.A., Novelli, P.C., Scranton, M.I., 1987. Methane oxidation and methane fluxes in the ocean surface-layer and deep anoxic waters. Nature 327 (6119), 226–229.
Weisenburg, D.A., Guinasso, N.L., 1979. Equilibrium solubilities of methane, carbon monoxide and hydrogen in water and seawater. Journal of Chemical Engineering Data 24, 354–360.
Weiss, R.F., 1970. The solubility of nitrogen, oxygen and argon in water and seawater. Deep-Sea Research 17, 721–735.
Weiss, R.F., Price, B.A., 1980. Nitrous-oxide solubility in water and seawater. Marine Chemistry 8 (4), 347–359.
Weiss, R.F., Van Woy, F.A., Salameh, P.K., 1992. Surface water and atmospheric carbon dioxide and nitrous oxide observations by shipboard automated gas chromatography: results from expeditions between 1977 and 1990. Scripps Institute of Oceanography Reference 92-11. ORNL/CDIAC-59, NDP-044. Carbon Dioxide Information Analysis Centre, Oak Ridge National Laboratory, Oak Ridge, Tennessee, 144pp.
Williams, P.J.L., Jenkinson, N.W., 1982. A transportable microprocessor-controlled precise winkler titration suitable for field station and shipboard use. Limnology and Oceanography 27 (3), 576–584.
Woodward, E.M.S., 2002. Nanomolar detection for phosphate and nitrate using liquid waveguide technology. Eos, Transactions American Geophysical Union 83 (4), 92, (2002 Ocean Sciences Meeting, published as supplement to Eos, Transactions American Geophysical Union).
Yelland, M.J., Moat, B.I., Taylor, P.K., Pascal, R.W., Hutchings, J., Cornell, V.C., 1998. Wind stress measurements from the open ocean corrected for airflow distortion by the ship. Journal of Physical Oceanography 28 (7), 1511–1526.
Yoshinari, T., 1976. Nitrous oxide in the sea. Marine Chemistry 4, 189–202.